Formation and Relaxation of Two-Dimensional Vortex Crystals in a Magnetized Pure-Electron Plasma

Y. Kiwamoto,* N. Hashizume, Y. Soga, J. Aoki, and Y. Kawai

Graduate School of Human and Environmental Studies, Kyoto University, Kyoto 606-8501, Japan

(Received 7 February 2007; published 12 September 2007)

Systematic examinations are carried out experimentally about the contribution of background vorticity distributions (BGVD's) to the spontaneous formation and decay of ordered arrays (vortex crystals) composed of strong vortices (clumps) by using a pure-electron plasma. It is found that the BGVD level needs to be higher for an increasing number of clumps to form vortex crystals and that the number of the clumps constituting the crystal decreases in time as $\propto \gamma \ln t$ in contrast to $\propto t^{-\xi}$ with $\xi \approx 1$ as accepted well in turbulence models. The decay rate γ increases with the BGVD level. The observed configurations of the clumps cover the theoretically predicted catalogue of vortex arrays in superfluid helium, suggesting a possible relaxation path of the crystal states.

DOI: 10.1103/PhysRevLett.99.115002 PACS numbers: 52.27.Jt, 47.32.ck, 52.25.Xz, 52.35.We

Morphological correspondence between the guiding-center flow of electrons in magnetized non-neutral plasmas and the two-dimensional (2D) Euler fluid allows translation of the electron density to the vorticity distribution of an incompressible 2D flow [1–3]. Many aspects of turbulence in high-Reynolds-number 2D fluids have been demonstrated with pure-electron plasmas, [3,4] including vortex merger and punctuated reduction of the vortex population that depends algebraically on time as $\propto t^{-\xi}$ with an exponent $\xi \approx 1$ as predicted by numerical simulations and scaling theories [5–8]. One of striking observations achieved by Fine *et al.* was the self-organization of crystals composed of strings of high-density electrons (clumps) in the relaxation process of the turbulence starting from unstable density distributions [4]. The corresponding dynamics was examined and confirmed by numerical simulations [9]. The observed clump configurations were reproduced theoretically by the regional maximum fluid entropy (RMFE) model under a given set of parameters [10].

It was observed that the number of crystallized clumps decreases in time while changing the geometrical configurations [4]. Stability of various configurations of the clumps' array were examined and compared with a catalogue of stable patterns of vortices in rotating superfluid helium [11,12]. The role of the background vorticity distribution (BGVD) was acknowledged to be crucial to the formation of crystals, though there have been only a few experimental examinations even on the configuration of a small number of clumps [13,14]. It should be noted that BGVD is influential also on the destruction of a crystal state that is followed by the next generation of crystal. Such dynamical relaxations of crystal states have not been under quantitative experimental examinations.

The purpose of this Letter is to examine the vortex dynamics that includes generation of vortex crystals and destructive transition to another configuration by carefully taking the role of BGVD into consideration. Because the relaxation process is stochastic in nature, high reproducibility is required in preparing the initial distributions. In contrast to the experiment by Fine *et al.* that was not free from shot-by-shot variations in the initial vorticity distribution of instability origin, the present experiment employs highly controlled initial distributions that do not depend on instabilities. The distributions of the clumps and the background population are generated separately and superposed to form the initial state of the clumps-BGVD system.

This technique was employed previously to examine the dynamics of a small number of clumps mutually interacting via controlled level of BGVD [13–15]. Major contributions of the BGVD have been observed to lie in bifurcating fast merger and long-lasting separation between neighboring clumps [13] and in advecting three clumps to symmetric locations that constitute a unit cell of a crystal [14]. On the basis of understanding such basic processes the main concern of this Letter is to examine the evolution of a many-clump system in interaction with controlled amount of BGVD.

New findings to be reported here include the followings: A certain level of BGVD is required for a given number of clumps to form a crystal. If the initial BGVD is not high enough, the clumps decrease in number and remain random in distribution until the level of BGVD reaches a height required for the remaining clumps to form a crystal. The time of the crystallization depends on the number of the clumps. The experimental observations lead to an empirical relation between the clumps' number and the time of crystallization that is not algebraic but logarithmic in time. The observed configurations of the clumps reproduce most of the vortex patterns in the rotating superfluid helium as predicted theoretically to be in the minimum energy state [12].

The experiments are carried out in a Malmberg trap with the same configuration as previously reported [13–15]. Up

to 19 cathodes can be activated to generate string distributions of electrons (clumps) aligned parallel to the uniform magnetic field of $B_0 = 0.048$ T and to trap them in a square-well potential that is optimized to support the longest lifetime of the strings by adjusting the distribution of the bias voltages applied to the axially aligned ring electrodes functioning as a conducting wall.

A flat density profile of the BGVD is prepared by the operation including repetitive injection and trapping of electron beams followed by partial spilling out of the electrons in a relaxed state. The axial uniformity of the electron density distribution is confirmed by self-consistently solving the Poisson-Boltzmann equation [16]. Four levels of BGVD's are generated with the radial distribution as shown in Fig. 1. The initial number of electrons $N_b/10^8$ constituting the BGVD's is 0.7 (△), 1.4 (□), 1.8 (◇), 2.2 (○), each of which is labeled as BGVD1 to 4. The initial state with $N_b = 0$ is added as BGVD0 with a symbol of ▽. The average heights of BGVD 0 to 4 are 0, 0.5, 0.75, 1.2, 1.6×10^{12} m^{-3}, respectively. Clumps, each of which includes average number of 2.1×10^6 electrons, are injected in a single shot after the completion of the BGVD. The initial peak densities of the clumps are typically 40 times higher than that of BGVD4.

The observations are made by recording the luminosity distribution on a phosphor screen that shines at the wavelength of 610 nm on the arrival of electrons escaping over the depressed potential barrier after a prescribed time of holding in the trap and accelerated to 7.5 keV. The luminosity distribution recorded at 512×512 pixels of a charge-coupled-device camera represents the 2D distribution of the axially integrated electron density $nl(x, y)$. The proportionality between the electron number and the count at each pixel has been confirmed [17,18]. Based on the axial uniformity of the potential profile and the magnetic field, the electron density is evaluated as $n(x, y, z) = nl(x, y)/L$, where $L = 0.18$ m is the distance between the reflection points for the bulk electrons with temperature

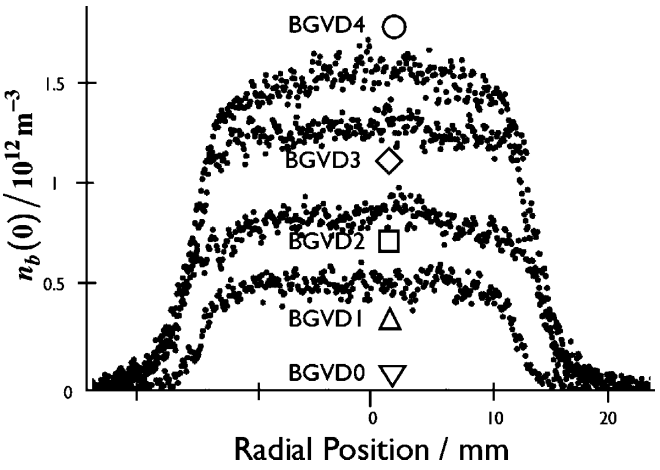

FIG. 1. Initial density distribution of background electrons acting as BGVD. The total number of electrons is $N_b/10^8 =$ 0.7 (△), 1.4 (□), 1.8 (◇), 2.2 (○).

of 1 eV. Using the morphological equivalence the electron density is related to the vorticity by $\zeta(x, y) = en(x, y, z)/\varepsilon_0 B_0 = enl(x, y)/\varepsilon_0 B_0 L$, where ε_0 is the dielectric constant of vacuum.

The time evolution of the clumps-BGVD system is examined by injecting an identical set of 14 clumps into the BGVD's 0 to 4. Examples of the 2D distribution $nl(x, y)$ after varied time of relaxation of the clumps in the BGVD4 are shown in Fig. 2. The clumps' distribution at $t = 0$ ms is common to all the data presented in this Letter. The clumps move chaotically during the initial 1 ms. The first array that may barely be considered to be a crystal appears at $t =$ 0.9 ms with 12 clumps. As the relaxation proceeds other crystal configurations appear with decreasing number of clumps. It is quite rare in the time domain of $t > 1$ ms that disordered distributions are observed. The statistics indicate that the average lifetime of crystal states is much longer than the duration of occasional turbulent states in which clumps move chaotically to merge shedding out filamentary structures of tenuous population that eventually join the BGVD.

The number of clumps $\tilde{n}_c$ that form ordered arrays in different levels of BGVD are plotted in Fig. 3 as a function of time. When the clumps are injected in vacuum (BGVD0) the first crystal appears with three clumps after 10 ms of relaxation. It means that 11 clumps are destroyed to form the BGVD that is necessary to settle down the remaining 3 clumps at the vertices of an equilateral triangle [9,14]. At the lowest level of the BGVD1 the first crystal appears with 4 clumps. As the initial level of BGVD increases the number of the clumps forming the initial crystal increases and the time required for the crystallization decreases.

Though the initial distributions are adjusted to be highly reproducible, within a few percent, there is substantial scatter in the plotted data, indicating chaotic dynamics of the clumps in interaction with the fluctuating BGVD. In the linear plot of the number of clumps $\tilde{n}_c(t)$ against the logarithmic scale of time t one can draw linearly decreasing regression lines around which most of the data points are distributed, while they are scattered around a convex curve in a log-log diagram. The fitting lines may be written in the form

$$\tilde{n}_c(t) = \tilde{n}_c(t_0) - \gamma \ln(t/t_0). \quad (1)$$

Here t_0 stands for the time the first crystal appears with $\tilde{n}_c(t_0)$ clumps.

The decay coefficient γ increases with the height of BGVD. Open symbols in Fig. 4 show γ as a function of the initial density $n_b(0)$ of BGVD in the unit of 10^{12} m^{-3}. A more meaningful presentation may be given by the closed symbols representing the density $n_b(t_0)$ at the generation of the first crystal. Because the observation indicates that the height of BGVD does not change at $t \geq t_0$, γ determined at $t = t_0$ remains approximately unchanged at $t > t_0$. The solid line of regression drawn in Fig. 4 for the

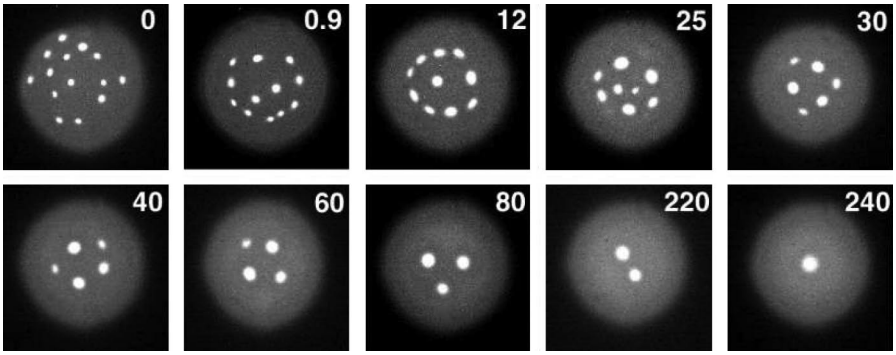

FIG. 2. Time history of the distribution of 14 clumps injected into the BGVD4. Brightness indicates the height of the density or vorticity distributions. The attached numbers represent the time (in ms) of observation after the injection of the clumps.

closed symbols may be written as

$$\gamma = 0.166 \exp[1.613 n_b(t_0)], \tag{2}$$

or

$$\gamma = 0.166 \exp[4.3 \times 10^{-6} \zeta_b(t_0)], \tag{3}$$

in terms of the vorticity $\zeta_b(t_0)$ in the unit of s^{-1}.

The new empirical formula (1) differs clearly from the power-law scaling of $\tilde{n}_c(t) \propto t^{-\xi}$ that fits to the decreasing number of vortex patches in turbulent states as examined by numerical simulations [5–7] and by pure-electron plasma experiments [4]. In view of the new scaling we replot the data points at $t > \tau_R$ in Fig. 3 of Ref. [4] representing the crystal states in the semilog diagram as shown in the inset of Fig. 3. The data points are distributed more orderly around a straight line than in the original log-log diagram, so that these data also support the logarithmic scaling. Since our experiment also supports the power-law scaling in the reducing number of clumps before crystallization, it may be concluded that the number of strong vortices follows the power-law scaling in the turbulent stage and switches to the logarithmic scaling after the appearance of the first crystal.

Let us relate the logarithmic scaling (1) to the power-law scaling and discuss its implication. If we introduce the normalized time $\tau = t/t_0$, the reduction rate of the clumps' number is rewritten as

$$\frac{d\tilde{n}_c(\tau)}{d\tau} = -\gamma \exp\left[-\frac{\tilde{n}_c(1) - \tilde{n}_c(\tau)}{\gamma}\right]. \tag{4}$$

Introduction of the Boltzmann-type transformation $\eta = \exp[\tilde{n}_c/\gamma]$ that includes contributions both from the clumps and from BGVD leads to

$$\eta_1 \frac{d\eta}{d\tau} = -\eta^2 = -\frac{d}{d\eta} U(\eta), \tag{5}$$

which describes the relaxation of the state function $\eta(\tau)$ in terms of the displacement of a quasiparticle slipping down the potential $U(\eta) = \eta^3/3$ with a frictional coefficient of

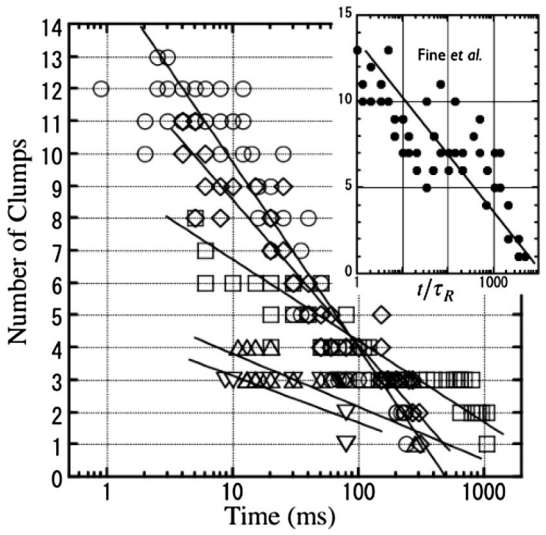

FIG. 3. Number of clumps constituting vortex crystals is plotted against the logarithmically-scaled relaxation time. Symbols correspond to the initial BGVD as shown in Fig. 1. Aggregates of more than 10 pixels are considered as clumps only when the count on each pixel exceeds the BGVD level by more than 3 times of the fluctuation level in BGVD. The inset replots the data by Fine *et al.* [4].

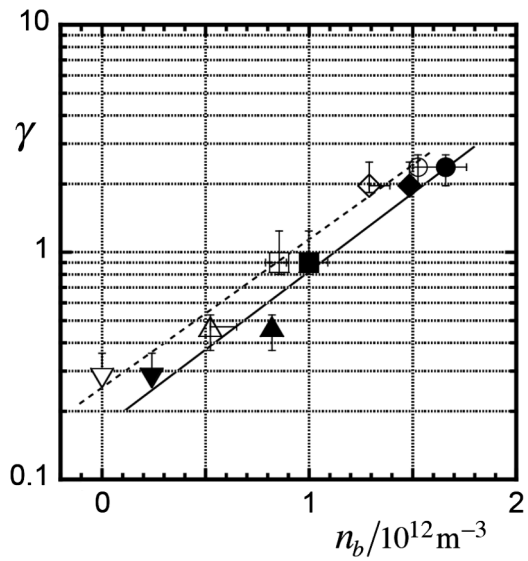

FIG. 4. Decay coefficient of the clumps' number plotted as a function of the height of BGVDs. Symbols correspond to the initial BGVD as shown in Fig. 1. The open symbols stand for the initial state and the closed symbols represent the BGVD at $t = t_0$ when the first crystal appears. The size of the symbols without bars includes the variance of data.

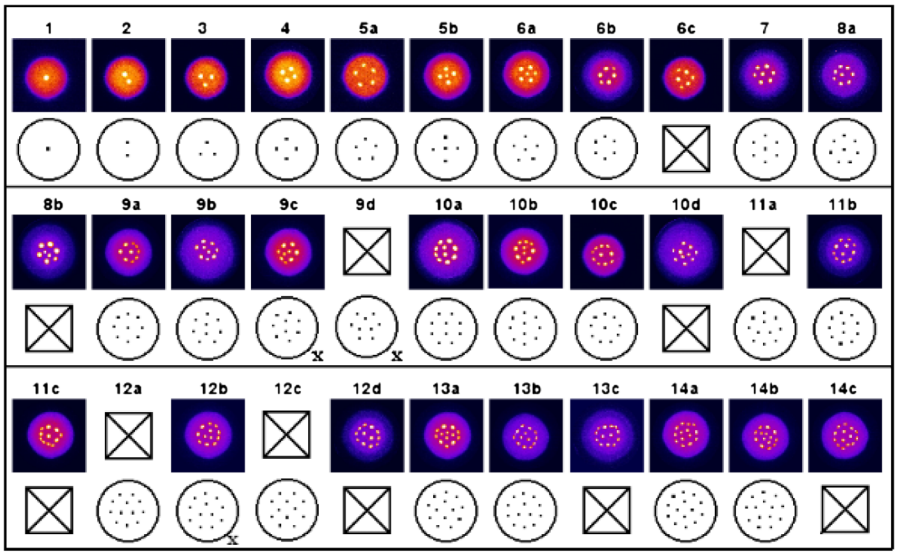

FIG. 5 (color online). Image of the vortex crystals observed in the pure-electron plasma starting with 14 clumps (upper panels). Compared are theoretically predicted 2D arrays of vortex strings in liquid helium (lower panels). The symbol ⊠ indicates the absence of observation or of prediction. The symbol "x" indicates the state is metastable in theory.

$\eta_1 = \eta(1)$. The solution of Eq. (5) satisfies the power-law scaling of $\eta(\tau) = \eta_1 \tau^{-\xi}$ with $\xi = 1$. The frictional drift may be interpreted in terms of trapping and detrapping of the quasiparticle in local minima (crystal states) of the effective potential $U(\eta)$ that is of rugged shape before being smoothed for the regression fitting.

The local-minimum-energy states were examined theoretically [12] to explore stable two-dimensional lattice configurations of vortex strings in a rotating cylindrical superfluid helium system stimulated by experimental observations [19]. Figure 5 compares the predicted configurations of the vortex strings with the crystal states of electron clumps observed in the present experiment. While the circulations of quantum vortices are forced to be the same, the classical electron vortices are allowed to be of different circulations. Slight discrepancies are attributable to the nonuniformity of electron circulations in the experiment. A good agreement between the theory and the observations supports the physical picture that electron clumps track minima of a effective potential composed by the clumps and BGVD though it does not necessarily exclude the validity of RMFE theory.

In summary, on the basis of the present and previous experiments, the relaxation of the crystal states may be understood as follows: The BGVD has a positive role in advection of clumps into a symmetric configuration and in keeping the crystal state stable [11,13,14]. For this role to be active BGVD has to be above a certain level. Once a crystal is formed, the configuration remains quasistationary until some of the clumps are quenched by some dissipative processes likely to be associated with local shears due to the surrounding BGVD. The disappearance of a clump breaks the stable configuration and triggers turbulent vortex dynamics that may include mergers of clumps and last until a new stable configuration is reached in BGVD.

This research was supported by the Grant-in-Aid for Scientific Research (B) No. 17340173 of JSPS and partly by the collaborative program of NIFS.

*kiwamoto@mbox.kudpc.kyoto-u.ac.jp
http://plasma.jinkan.kyoto-u.ac.jp

[1] R. H. Levy, Phys. Fluids **11**, 920 (1968).
[2] R. J. Briggs, J. D. Daugherty, and R. H. Levy, Phys. Fluids **13**, 421 (1970).
[3] C. F. Driscoll and K. S. Fine, Phys. Fluids B **2**, 1359 (1990).
[4] K. S. Fine, A. C. Cass, W. G. Flynn, and C. F. Driscoll, Phys. Rev. Lett. **75**, 3277 (1995).
[5] J. C. McWilliams, J. Fluid Mech. **219**, 361 (1990).
[6] G. F. Carnevale, J. C. McWilliams, Y. Pomeau, J. B. Weiss, and W. R. Young, Phys. Rev. Lett. **66**, 2735 (1991).
[7] J. B. Weiss and J. C. McWilliams, Phys. Fluids A **5**, 608 (1993).
[8] U. Frisch, *Turbulence* (Cambridge University Press, Cambridge, England, 1995).
[9] D. Schecter, D. H. E. Dubin, K. S. Fine, and C. F. Driscoll, Phys. Fluids **11**, 905 (1999).
[10] D. Z. Jin and Daniel H. E. Dubin, Phys. Rev. Lett. **80**, 4434 (1998).
[11] D. Durkin and J. Fajan, Phys. Fluids **12**, 289 (2000).
[12] L. J. Campbell and R. M. Ziff, Phys. Rev. B **20**, 1886 (1979).
[13] Y. Soga, Y. Kiwamoto, and A. Sanpei, Phys. Plasmas **10**, 3922 (2003).
[14] A. Sanpei, Y. Kiwamoto, K. Ito, and Y. Soga, Phys. Rev. E **68**, 016404 (2003).
[15] Y. Kiwamoto, K. Ito, A. Sanpei, and A. Mohri, Phys. Rev. Lett. **85**, 3173 (2000).
[16] J. Aoki, Y. Kiwamoto, and Y. Kawai, Phys. Plasmas **13**, 112109 (2006).
[17] K. Ito, Y. Kiwamoto, and A. Sanpei, Jpn. J. Appl. Phys. **40**, 2558 (2001).
[18] J. Aoki, Y. Kiwamoto, Y. Soga, and A. Sanpei, Jpn. J. Appl. Phys. **43**, 7267 (2004).
[19] E. J. Yarmchuk, M. J. V. Gordon, and R. E. Packard, Phys. Rev. Lett. **43**, 214 (1979).